Structural Engineering and Mechanics, *Vol. 72, No. 1 (2019) 83-97*
DOI: https://doi.org/10.12989/sem.2019.72.1.083

Studying the Park-Ang damage index of reinforced concrete structures based on equivalent sinusoidal waves

Moosa Mazloom*[1], Pardis Pourhaji[2], Masoud Shahveisi[1] and Seyed Hassan Jafari[1]

[1]*Department of Civil Engineering, Shahid Rajaee Teacher Training University, Tehran, Iran*
[2]*Department of Civil Engineering, Iran University of Science and Technology, Tehran, Iran*

(Received June 7, 2018, Revised April 28, 2019, Accepted May 7, 2019)

Abstract. In this research, the vulnerability of some reinforced concrete frames with different stories are studied based on the Park-Ang Damage Index. The damages of the frames are investigated under various earthquakes with nonlinear dynamic analysis in IDARC software. By examining the most important characteristics of earthquake parameters, the damage index and vulnerability of these frames are investigated in this software. The intensity of Erias, velocity spectral intensity (VSI) and peak ground velocity (PGV) had the highest correlation, and root mean square of displacement (D_{rms}) had the lowest correlation coefficient among the parameters. Then, the particle swarm optimization (PSO) algorithm was used, and the sinusoidal waves were equivalent to the used earthquakes according to the most influential parameters above. The damage index equivalent to these waves is estimated using nonlinear dynamics analysis. The comparison between the damages caused by earthquakes and equivalent sinusoidal waves is done too. The generations of sinusoidal waves equivalent to different earthquakes are generalized in some reinforced concrete frames. The equivalent sinusoidal wave method was exact enough because the greatest difference between the results of the main and artificial accelerator damage index was about 5 percent. Also sinusoidal waves were more consistent with the damage indices of the structures compared to the earthquake parameters.

Keywords: damage index, particle swarm optimization, earthquake parameter, reinforced concrete structures

1. Introduction

Earthquakes are natural and probable subjects that human beings have been struggling with for a long time (Mohebi et al. 2019). The only thing can be done is to identify the basic parameters of earthquakes more precisely and strengthen buildings (Cantagallo et al. 2019). In recent years, many improvements has been made in the retrofitting of structures (Habibi A. Izadpanah M. 2012, Habibi A.R. et al. 2013 and Rahman M. S. et al. 2017). The assessment of the damages caused by earthquakes and the vulnerability of structures were the results of these researches. It should be kept in mind that structures cannot be designed to have no damage in earthquakes (Habibi A. and Asadi K. 2017). Considering different factors in the design, it is possible to create different modes of damages in the structures during earthquakes (Bas S. and Kalkan I. 2016). Nowadays, sustainability in construction has attracted a lot of attention (Zarghami et al. 2017 and Zarghami et al. 2018). In this regard, new generations of concrete such as self-compacting lightweight concrete have been introduced (Karamloo et al. 2017). It improves the sustainability and diminishes the deteriorative effects regarding the use of normal concrete (Mazloom et al. 2015, Mazloom and Mahboubi 2017 and Mazloom and Ranjbar 2010). Moreover, recently, there have been suggestions for evaluating the structural damages caused by earthquakes, which can help to make decisions in the field of retrofitting of structures. In fact, assessing the seismic vulnerability of existing buildings is a prediction of their damages for possible earthquakes (Ozmen H. B. and Inel M. 2016). Qualitative methods, despite their low accuracy, are still used in estimating seismic hazards of cities and statistical studies of buildings. These methods have been widely developed in countries like Japan (Kim and Chung 2016).

Quantitative methods gradually replaced the qualitative ones and complemented them. Computer software programs such as DRAIN can do nonlinear analysis of frames (Basack S. and Nimbalkar S. 2017). Also, ACE, DAEM and DAMAGE software can evaluate the seismic resistance of frames (Chen et al. 2017). This method was applicable to all buildings, and depended on the type of resistant elements, the strength of structural joints, the inter structure loads, the presence or absence of structural coils or structural ratios, and possible changes in these parameters. Spatial matrix spectroscopy method, which is to estimate the damage potential of a building or a group of them, expressed the characteristics of earth moving during earthquake with using a speed response spectrum (FEMA 2000). Structural capacity in this method was described with base shear at the yield point, and the spin velocity was calculated against the base shear. The total damage was calculated as the ratio of repairs cost to the total reconstruction cost of the building. In this regard, an incomplete relationship was also presented with the coefficient of defeat (FEMA-356 2000). According to the effect of fatigue on the structure response,

*Corresponding author, Associate Professor
E-mail: Mazloom@sru.ac.ir

http://www.techno-press.com/journals/sem&subpage=7 ISSN: 1225-4568 (Print), 1598-6217 (Online)

Reinhorne et al. (1996) proposed a relationship for low cycle loadings. Studies had been carried out on concrete frames and mountain tunnels based on damage index (Chen et al. 2012, Vui and Raonagh 2014). In the Kapos report, the energy loss section included a very small proportion of damage indicators for well-designed structures. Therefore, their seismic damage assessment was more likely to be based on the degree of ductility (Kappos 1997). In addition, Colver et al. (1980) did the same. They used a computer program to take into account the exact response of the underlying earth structure. In their assessment method of the safety of buildings, the criterion of damage was determined by engineering judgments (Colombo and Negro 2005).

Banon and Veneziano (1982) presented a more advanced model for the evaluation of structural damage. In this method, damage was expressed on the basis of a two-dimensional rupture level of total energy absorbed and the ratio of absorbed damage. These models did not fully take into account the nonlinear behavior of reinforced concrete (RC) members under cyclic loads. Also, the effects of cutting and sliding reinforcement were ignored. Therefore, a weak relationship was found between the computational capacity of the structure and the failure of the tested ones in their model. Park et al. (1988) presented a new method in this field, which is called damage index. Considering a more comprehensive model for the nonlinear behavior of structures, members of it intervened in the damages to the building. In this way, the vulnerability calculations improved (Park et al. 1988). Park and Ang (1985) proposed a linear function of maximum deformation and cyclic load effected to assess the structural damage of buildings. The function proposed by them was the basis of work in IDARC software to evaluate the damage of RC frames. Izadpanaha M. and Habibi A. (2015) were used the IDARC program for inelastic analysis of reinforced concrete frames. Other researchers, such as Housner and Jennings (1964), continued to study using the substrate function and definition of various filters. Hajela and Berke (1991) determined an optimum weight for a truss to investigate the neural computing role in structural engineering.

By passing the time, some researchers proposed different methods to improve the calculation of earthquake parameters and the effects of earthquakes on structures (Artar M. 2016 and Chen and Yu 2017). Damage detection goes hand in hand with the structural reliability. Structural reliability algorithms such as non-negative constraint method (Roudak and Karamloo 2019), generalized Hasofer-Lind-Rackwitz-Fiessler method (Roudak et al. 2017), and other notable approximation methods uses different numerical techniques to find reliability index and probability of failure (Shayanfar et al. 2017, Roudak et al. 2018 and Roudak et al. 2017). For example, in the study conducted by Cantagallo et al. (2019), the probabilistic view point is added to the concept of damage index. In the last decade, Erdem (2010) predicted the critical moment capacity of the RC slabs in fire with the use of artificial neural networks (ANN). Jakubek (2017) calculated the load capacity of reinforced concrete columns using ANN. Lagaros and Papadrakakis (2012) investigated a nonlinear behavior of three-dimensional structures based on ANN adaptive scheme under severe earthquakes. Plevris and Papadrakakis (2011) exerted the structural optimization problems by using the enhanced PSO algorithm with a gradient-based on quasi-Newton sequential quadratic programming (SQP) technique. The particle swarm optimization (PSO) algorithm explored the design space detected the neighborhood of the global optimum (Mirzai et al. 2017). Subsequently, a nonlinear weight update rule and a constraint management method were proposed for PSO method and structural optimization respectively (Chen Z. and Yu L. 2017). The numerical results of this suggestion confirm its ability to recommend better solutions for structural optimization problems compared to other optimization algorithms (Chatterjee et al. 2016).

Moreover, researchers always pointed to the importance of correlation between earthquake parameters and building damage (Alvanitopoulos et al. 2010 and Habibi and Jami 2017). The response of reinforced concrete frames was expressed by the greatest relative displacement of the building. The total damage index was investigated in structures by Elenas and Meskouris (2001), Elnas (2000), Elenas (1997), Elenas and Liolios (1995), and Elenas et al. (1995). They concluded the energy and spectral parameters had the highest correlation with damage index, and peak ground acceleration (PGA) had the lowest correlation with it. In one of the previous researches, Vui and Raonagh (2014) concerned on the correlation between several earthquake parameters and structural damage of normal concrete structures. It was concluded that spectral velocity intensity had the highest correlation with structural damages.

The motivation of this research is to find a better way for calculating damage index of structures in an optimized time and high level of accuracy in comparison with other methods. In recent years, particle swarm optimization method is considered by civil engineers. It is a new algorithm to simulate equivalent characters, and the use of them in both design and analysis of structures. In this research, Park-Ang damage index was used to evaluate the damages of three, five and seven story frames with IDARC software. To verify the utilized software, some numerical examples were evaluated from earlier investigations, and the results confirmed the accuracy of the proposed software (Izadpanah and Habibi 2018 and Habibi and Izadpanah 2017). Then, particle swarm optimization algorithm was used to simulate the selective earthquakes with sinusoidal waves. The damage index was calculated according to equilibrium accelerations of the structures. Moreover, the correlation of earthquake parameters were investigated with Park-Ang damage index based on the main earthquakes. At the end of the research, all the results from these methods were compared to each other and an optimized one was chosen, which not only saved the design and analysis time but also its accuracy was acceptable.

2. Calculation of damage index

In IDARC software, the damage index, provided by Park-Ang, can be calculated (Valles et al. 1996). In this model, the damages are cumulative in all members of structures. The damages of structures are quantified by Damage Index (D), which indicates the damages caused by an earthquake as a linear combination of deformation) δ_m (and the absorbed hysteretic energy ($\int dE$) as follows.

$$D = \frac{\delta_m}{\delta_u} + \frac{\beta}{\delta_u P_u} \int dE \tag{1}$$

Where δ_m is the maximum deformation due to an earthquake, δ_u is ultimate deformation, β is resistance reduction parameter, P_y is yield strength, and $\int dE$ is absorbed hysterical energy. The damage index of the whole structure should be calculated according to the partial damage index (D_i) as presented in Eqs. (2)-(3).

$$\lambda_i = \frac{E_i}{\sum E_i} \tag{2}$$

$$D = \sum \lambda_i D_i \tag{3}$$

Where λ_i is the energy Weight Coefficient and E_i is the energy absorbed in each member.

3. Particle swarm optimization (PSO)

Kennedy and Eberhart (1995) were the main owners of the idea behind the PSO algorithm. Chaterjee et al. (2016) searched the creation of a robust algorithm for optimization, called particle swarm optimization algorithm or PSO. In PSO algorithm, there are a lot of organisms that are referred as particles, and distributed in the search space of the optimized function. Each particle calculates the value of target function in the located space position. Then, using the combination of its current location and the best place being in the past, as well as some information of the best particles in the total space, it chooses a direction to move. All particles have a direction for propagation, and after completing the movement, a phase of the algorithm ends. These steps are repeated several times until the desired result is obtained. This algorithm searches for the minimum value of a function, acts like a bunch of birds looking for food.

Each particle in PSO algorithm consists of some vectors in the research space, including the current position of the particle (x^i), the particle velocity (v^i), and the best position it has ever experienced ($x^{i,best}$). In fact, x^i is a set of coordinates that represent the current position of the particle, and at each step of the algorithm, it is considered as the answer to the problem. If this position is better than the previous one, it will be stored in $x^{i,best}$. The value of f^i is the objective function in x^i and $f^{i,best}$, the best value of the target function in $x^{i,best}$, both of these values are the constituent elements of each particle. Afterwards, each new iteration of x^i and v^i is achieved, and the purpose of implementing the algorithm is to improve $x^{i,best}$ and x^i possibly. The best position found by the particles is shown in x^{best}, which is selected by comparing the $f^{i,best}$ values for all particles and among the x^i. The value of the target function in x^{gbest} is shown by $f^{i,best}$. If the number of particles in the population is n, Eqs.(4)-(7) can be used for calculations in the algorithm.

$$x^{i,best}[t] = arg \min_{\tau \leq t} \{f(x^i[t]), f(x^{i,best}[t-1])\} \tag{4}$$

$$\begin{aligned} f^{i,best}[t] &= f(x^{i,best}[t]) \\ &= \min_{\tau \leq t} f^i[\tau] \\ &= \min \{f^i[t], f^{i,best}[t-1]\} \end{aligned} \tag{5}$$

$$x^{gbest}[t] = arg \min_{i=1,\dots,n} f(x^{i,best}[t]) \tag{6}$$

$$f^{gbest}[t] = f(x^{gbest}[t]) = \min_{i=1,\dots,n} f^{i,best}[\tau] \tag{7}$$

At the initial stage of the algorithm, particles are created with random positions and velocities. During the implementation of the algorithm, the position and velocity of each particle in the i+1 stage of the algorithm are constructed from the previous stage of information. If z_j is the j component of the vector z, the relations that change the speed and position are shown in Eqs. (8)-(9):

$$\begin{aligned} v_j^i[t+1] = w v_j^i[t] &+ c_1 r_1 \left(x_j^{i,best} - x_j^i[t]\right) \\ &+ c_2 r_2 (x_j^{gbest}[t] - x_j^i[t]) \end{aligned} \tag{8}$$

$$x_j^i[t+1] = x_j^i[t] + v_j^i[t+1] \tag{9}$$

In these equations, the coefficient of inertia is shown by ω. The values r_1 and r_2 are random numbers in interval [0, 1] with uniform distribution. Also c_1 and c_2 are learning coefficients. The values r_1 and r_2 make a variety of answers for the problem; therefore, a complete search happens on the investigation space. The value c_1 is the learning factor related to the personal experiences of each particle, and parameter c_2 is the coefficient of learning which is related to the total number of experiences. From Eq. 8, it can be concluded that for each particle in motion, the followings should be taken into account: (a) its previous motion, (b) the best position in which it was located, and (c) the best position experienced by the entire pluralist (Chaterjee et al. 2016).

4. Design of reinforced concrete frames

The methodology of this research shows the research process step by step (Fig. 1). Some RC frames were designed based on the Iranian earthquake building code (standard No. 2800-05). Also, the effects of earthquake parameters on the damage rate of reinforced concrete (RC) structures were considered by the authors

For this purpose, some three, five and seven story frames were selected. The studied buildings were designed with the assumption of satisfying intermediate ductility regulations. The structures were designed for Type 1 and Type II soils ductility of the Iranian earthquake building code.

Table 1 Selected earthquake characteristics in the first part for analysis in soil type I

Earthquake characteristics	Transvers wave			Longitudinal wave		
Earthquake name	Tabas	Aab bar	Vandik	Tabas	Aab bar	Vandik
Mean Period (T_m)	0.127	0.235	0.22	0.231	0.115	0.231
Predominant Period (T_p)	0.16	0.1	0.22	0.218	0.1	0.24
A95 Parameter	0.287	0.389	0.259	0.16	0.323	0.309
Effective Design Acceleration (EDA)	0.25	0.245	0.242	0.247	0.21	0.284
Sustained Maximum Velocity (SMV)	6.83	7.38	8.498	0.215	7.32	10.126
Sustained Maximum Acceleration (SMA)	0.149	0.319	0.241	5.881	0.291	22.32
Velocity Spectrum Intensity (VSI)	32.11	32.104	44.24	0.139	27.38	43.45
Acceleration Spectrum Intensity (ASI)	0.158	0.201	0.244	29.86	0.159	0.221
Cumulative Absolute Velocity (CAV)	0.386	0.699	0.672	0.172	0.702	0.68
Specific Energy Density (SED)	41.26	48.083	86.58	0.458	63.57	108.55
Characteristic Intensity(Ic)	0.0195	0.049	0.042	43.199	0.047	0.042
Erias Intensity (I_{Erias})	0.273	1.12	0.792	0.025	1.089	0.794
Displacement RMS	4.097	0.65	11.99	0.387	11.18	1.75
Velocity RMS	1.036	0.849	1.41	2.54	0.977	1.57
Acceleration RMS	0.0214	0.033	0.0343	1.06	0.32	0.034
V_{max}/A_{max}	31.78	21.49	36.306	0.025	26.36	35.38
Maximum Displacement (PGD)	8.608	6.52	17.891	35.94	21.53	2.86
Maximum Velocity (PGV)	9.15	8.474	9.54	3.55	8.63	11.05
Maximum Acceleration (PGA)	0.287	0.394	0.262	8.95	0.32	0.31

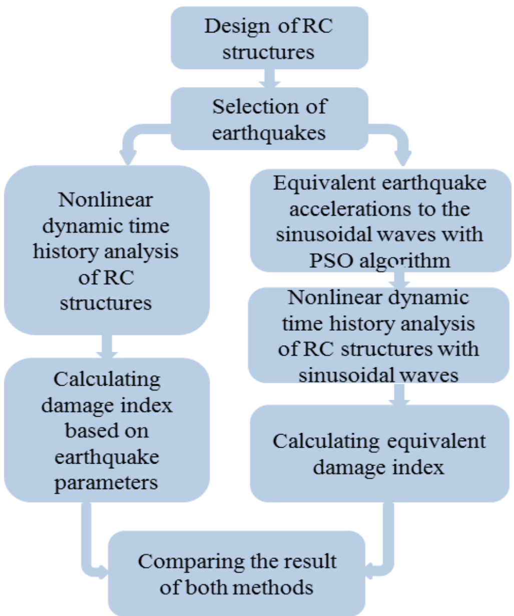

Fig. 1 The research methodology

Structural analyses were carried out using five kinds of structural elements. They were typical beams, edge beams, columns, shear walls, and the boundary elements of shear walls. The typical beams were modeled as flexural springs, in which shear deformations were also considered with an equivalent spring. The edge beams were modeled as elements having a degree of vertical freedom and a degree of torsional freedom. In the columns, axial deformations were considered. Shear walls were modeled as combinations of flexural and shear springs.

In this research, the compressive strength of concrete and yield strength of reinforcement were 25 MPa and 400 MPa respectively. A three-line model (reduction of strength, reduction of stiffness and narrowing) was used to model the hysteresis and nonlinear behavior of reinforced concrete.

As shown in Figs.1-3, in order to investigate the vulnerability of the studied buildings, the selected frames have been modeled in IDARC software for nonlinear dynamics analysis. The results of computational periods were presented using the ETABS and IDARC software as well as the experimental period calculated according to the Iranian earthquake building code (standard No. 2800-05). For the design of structures in type 1 and 2 soils, the element sections of the structures were constant, and with the change in the size of the rebar, the stress ratios were kept in acceptable limits.

5. Selection of earthquakes

In this study, 22 accelerators were utilized. At first, the correlation coefficient of earthquake parameters with damage index from 16 other accelerations was used similar to the previous one. These earthquakes included different accelerometers.

In the second step, six accelerators with two horizontal and vertical components of Iran earthquakes were selected in the database of building and housing research center (www.bhrc.ac.ir). In this regard, the longitudinal and transverse components of the three earthquakes of Tabas, Aab bar and Vandic have been selected in soil type I and

Table 2 Selected earthquake characteristics in the first part for analysis in soil type II

Earthquake characteristics	Transvers wave			Longitudinal wave		
Earthquake name	Naghan	Avaj	Chalan cholan	Naghan	Avaj	Chalan cholan
Mean Priod (T_m)	0.256	0.45	0.304	0.282	0.74	0.24
Predominant Priod (T_p)	0.24	0.24	0.12	0.2	0.24	0.1
A95 Parameter	0.48	0.352	0.21	0.492	0.42	0.28
Effective Design Acceleration (EDA)	0.439	0.353	0.164	0.423	0.41	0.148
Sustained Maximum Velocity (SMV)	19.06	20.78	13.35	28.16	38.69	24.98
Sustained Maximum Acceleration (SMA)	0.371	0.31	0.141	0.392	0.307	0.108
Velocity Spectrum Intensity (VSI)	64.36	145.5	41.09	83.04	173.49	33.06
Acceleration Spectrum Intensity (ASI)	0.4	0.369	0.132	0.44	0.323	0.119
Cumulative Absolute Velocity (CAV)	0.795	1.14	0.309	0.942	1.096	0.285
Specific Energy Density (SED)	1670	1245.4	1511.3	3006.5	3152.05	5101.89
Characteristic Intensity(I_c)	0.059	0.0604	0.0203	0.074	0.056	0.019
Erias Intensity (I_{Erias})	1.406	1.642	0.236	1.862	1.489	0.22
Displacement RMS	174.5	58.07	76.87	235.72	133.11	170.29
Velocity RMS	5.32	3.701	8.48	7.145	5.88	16.38
Acceleration RMS	0.039	0.034	0.027	0.045	0.0326	0.0274
V_{max}/A_{max}	49.46	108.26	65.17	71.17	95.105	94.85
Maximum Displacement (PGD)	254.8	75.8	152.88	342.22	172.35	293.38
Maximum Velocity (PGV)	23.94	38.68	13.85	35.503	41.07	26.63
Maximum Acceleration (PGA)	0.484	0.357	0.212	0.498	0.431	0.28

three Naghan, Avaj and Chalan Cholan earthquakes were chosen in soil type II. The results of the research were generalized for the seismic design of concrete structures having intermediate ductility conditions. The equation of acceleration of various earthquakes was replaced by sinusoidal waves. Then, the equivalent damage index was determined from the waves on the reinforced concrete structures. In Tables 1 and 2, the damages of the structures were plotted according to the Park-Ang damage index and seismic parameters.

5.1.1 Dynamic time history analysis

The results of dynamic nonlinear time histories analyses of the investigated structures are presented in this part. In fact, using the obtained results, the diagrams of the total damage indices of the structures are plotted in terms of different earthquake parameters. According to Elenas (1997), these parameters are maximum pseudo-acceleration (PGA), maximum ground speed (PGV), maximum ground displacement (PGD), maximum velocity ratio to maximum acceleration (V_{max} / A_{max}), root mean square acceleration (RMS acceleration), RMS velocity, RMS displacement, Erias intensity, characteristic intensity (I_c), specific energy density (SED), cumulative absolute velocity (CAV), acceleration spectrum intensity (ASI), velocity spectrum intensity (VSI), sustained maximum acceleration (SMA), sustained maximum speed (SMV), and effective design acceleration (EDA). Finally, the degree of correlations of these characteristics were achieved

The damage indices for each of the mentioned parameters were considered in eight different modes, and the correlation coefficients in each case were calculated. These eight types included soil type I - transverse wave, soil type I - longitudinal wave, soil type II- transverse wave, soil type II-longitudinal wave, soil type I, soil type II, longitudinal wave, transverse wave. In this way, a set of correlation coefficients for each of the parameters were obtained and discussed.

In the first step, the linear equations were fitted on the data and the correlation coefficients were calculated. If these coefficients were above 75%, they were assumed to be acceptable. If not, nonlinear equations were used, in this regard, to improve correlation coefficients. It is worth noting that, if the use of nonlinear equations did not lead to the increase of correlation coefficients, the linear correlation coefficients were used again. Based on the research of Elenas (1995), the method of calculating the correlation coefficients did not have significant effects on the degree of correlations. In the presented curves, the thick line refers to the 7-story buildings, the normal line is related to the 5-story building, and, finally, the thin line is for the three-story buildings.

5.1.2 Analysis of the results on earthquake parameters

The most common way to study the effects of earthquake ground motions on structures is to use time history analysis. The direct use of earthquake accelerations is very time consuming, and the interpretation of the results is difficult. In fact, the dispersion of the results does not allow the researchers for proper explanation. Therefore, it is common in practice to introduce an earthquake with a

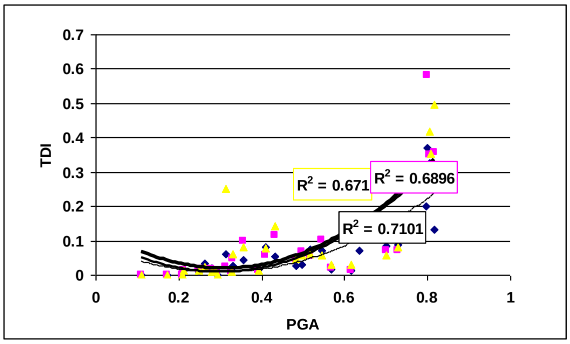

Fig. 2 Total Charts for damage index in PGA

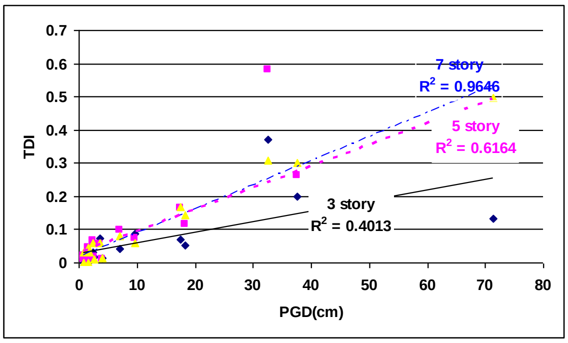

Fig. 4 Total Charts for damage index in PGD

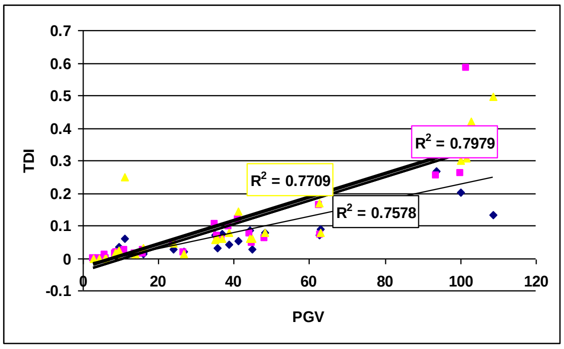

Fig. 3 Total Charts for damage index in PGV

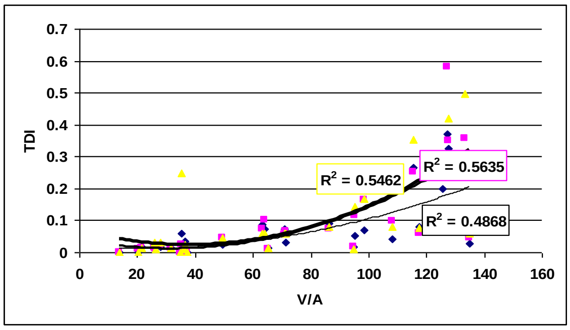

Fig. 5 Total Charts for damage index in V_{max}/A_{max}

specific coefficient, and then to conduct an investigation based on that coefficient. The important thing is that these coefficients should be defined and selected to be the best representatives of the earthquakes. In other words, there is sufficient familiarity with the abilities and limitations of these definitions, so that the misconception of the results does not occur.

In earthquake engineering, many of the parameters are defined in order to study the structures against earthquakes. The parameters of the ground motion are based on the characterization of the maximum ground motion in a compact and qualitative manner. Many parameters are proposed for specifying the range, frequency, and duration of strong ground motions.

The relationships between intensity, acceleration, velocity, and sometimes displacement are the basis of design and retrofit of structures against earthquakes. The simplest expression for measuring the acceleration is to use peak ground acceleration (PGA). PGA method does not have any information about the duration and frequency of the earthquake. In order to eliminate this method, another measurement, which is root mean square (acceleration RMS or A_{rms}), is presented.

Peak ground acceleration (PGA)

The most common criteria for earthquake measurements are to study maximum values. For this parameter, the best fits were obtained using quadratic curves. Peak ground acceleration (PGA) is studied here (Steven L. Kramer 1996), and as the PGA increased, the damage index improved. Also, in this investigation, the damage index of the structures increased when the number of stories increased. The results of the total data for soils type I and II soils are shown in Fig. 2.

Peak ground velocity (PGV)

In this case, the linear curve fitting was sufficient, and the amounts of correlation coefficients were acceptable. In this regard, it can be said that with increasing peak ground velocity (Steven L. Kramer 1996), the damage indices of the structures increased linearly. In Fig. 3, the damage of taller structure was more than the smaller ones.

Peak ground displacement (PGD)

Linear curve fitting was exact enough for peak ground displacement (Steven L. Kramer 1996). In fact, Fig. 4 shows that with increasing PGD, the damage indices of the structures improved linearly. Also in almost all scenarios, the damage indices of taller structure were more than the shorter ones.

Maximum velocity to maximum acceleration ratio

Usually the maximum velocity and acceleration depend on different motion frequencies. Quadratic curve fitting were suitable in this case. According to Fig. 5, by increasing V_{max}/A_{max} (Steven L. Kramer 1996), the damage indices of the structures advanced with a quadratic relationship. In general, the structures with higher stories suffered from more damages.

Root mean square acceleration (A_{rms})

Factors reflect more than one character are very useful for resolving the problem of maximum motion parameters. They are introduced without communication with time and frequency. In fact, these factors measure the amount of

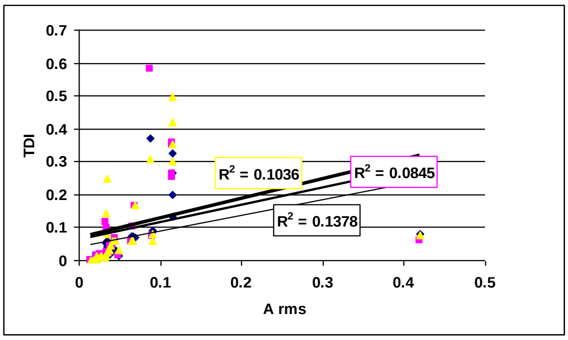

Fig. 6 Total Charts for damage index in A_{rms}

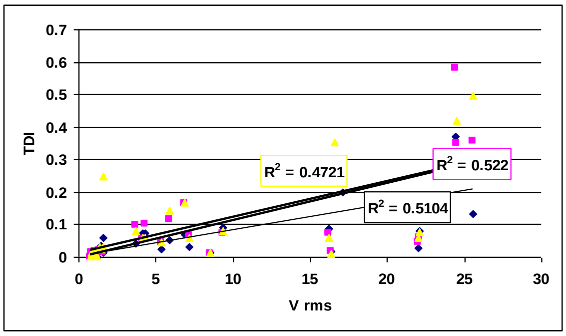

Fig. 7 Total Charts for damage index in V_{rms}

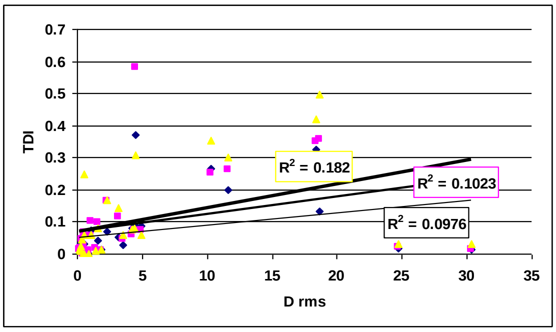

Fig. 8 Total Charts for damage index in D_{rms}

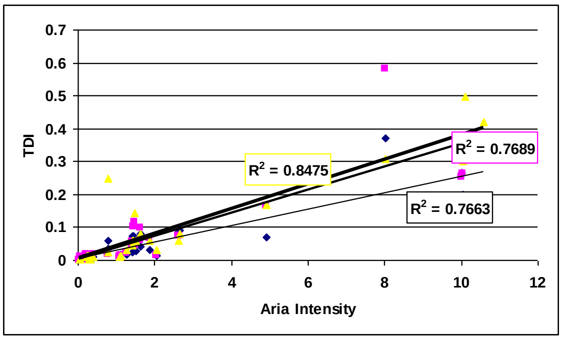

Fig. 9 Total Charts for damage index in I_{Erias}

energy in ground motions caused by an earthquake. Root mean square acceleration (A_{rms}) shows the amplitude and frequency effects of an earthquake record with a value. Based on this parameter, the speed and displacement of the RMS can also be defined. The A_{rms} is very useful for engineering purposes. If the wave is a sinusoidal earthquake, RMS parameters can be calculated with much simpler calculations (Steven L. Kramer 1996).

In this case, a linear curve fitting was sufficient. As shown in Fig. 6, it can be said that with increasing RMS, the damage index of the structures increased linearly. Also, in most cases, the damages of higher structures were more than the shorter ones.

Root mean square of velocity (V_{rms})

In this case, the linear curve fitting was sufficient. In this system, with increasing root mean square of velocity (Steven L. Kramer 1996), the damage indices of the structures increased linearly (Fig. 7). In this case, the damages of taller structures were not more than the shorter buildings necessarily.

Root mean square of displacement (D_{rms})

Neither linear nor nonlinear curve fittings were appropriate for introducing the damage indices in terms of root mean square of displacement (Steven L. Kramer 1996). In Fig. 8, a linear curve was used since the other curves did not have suitable correlation coefficients. The only thing can be said is that the growth of RMS displacement increased the damage indices slightly.

The intensity of Erias (I_{Erias})

The intensity of Erias is measured according to the ground motion acceleration. This parameter is defined as an integral in the natural energy frequency range of the input to the single degree of freedom system, and the degree of freedom in the acceleration response. In other words, this parameter is the criterion for determining the total energy absorption of earthquakes by the earth. It is equal to the total energy absorbed by the vibrometers too. In fact, Erias is one of the best criteria for earthquake measurement. It has a positive correlation with damage index in low period structures. Also, this criterion is very useful in predicting landslide and liquefaction (Steven L. Kramer 1996).

In this case, as shown in Fig. 9, the linear curve fitting was appropriate. In other words, with increasing the intensity of Erias, the damage indices of the structures increased linearly.

Characteristic intensity (I_c)

Characteristic intensity (Massumi and Gholami 2016) is a quantity that shows the failure potential of earthquakes. Damage index has a linear relationship with deformation and adsorbed hysteresis energy. According to Fig. 10, as the I_c increased, the damage index increased linearly. This figure shows that the results of I_c values were very close, and it was not possible to distinguish between damage indices in different soils and waves.

Special energy density (SED)

Calculation of special energy density (Steven L. Kramer 1996) is shown in Eq.10. Linear curve fitting was sufficient in this case. In other words, with increasing energy density, the damage index increased linearly (Fig. 11). This parameter had no sensitivity to the height of the structures.

$$SED = \int_0^{t_s} [v(t)]^2 \, dt \qquad (10)$$

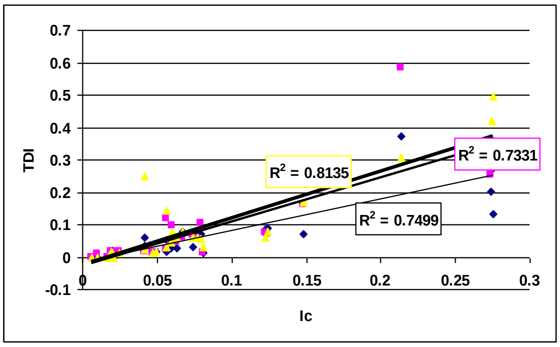

Fig. 10 Total Charts for damage index in I_c

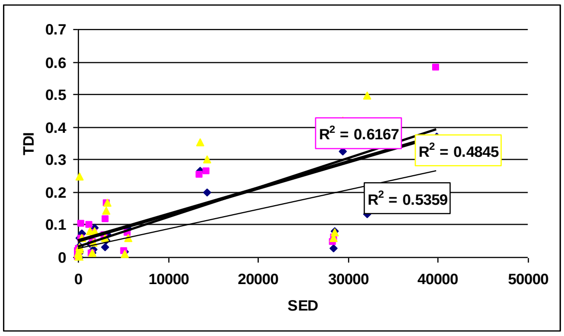

Fig. 11 Total Charts for damage index in SED

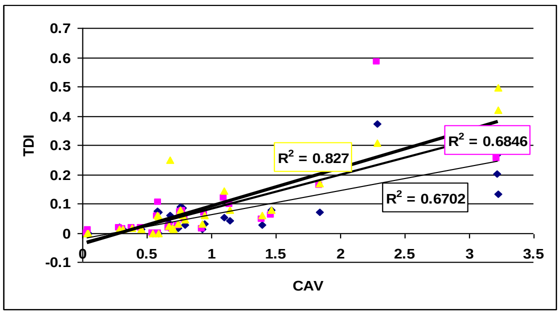

Fig. 12 Total Charts for damage index in CAV

Cumulative absolute velocity (CAV)

The cumulative absolute velocity is equal to the surface under the curve of the magnitude of the acceleration (Cabanas L. et al. 1997).

Linear curve fitting was used in this case. It means, with increasing cumulative acceleration, the damage index increased linearly. This parameter was slightly sensitive to the height of the structures, and as the cumulative velocity increased, the damage index in the taller structures raised (Fig. 12).

Acceleration of Spectral intensity (ASI)

The calculation of the acceleration of spectral intensity is shown in Eq.11. S_a is spectral acceleration, dT is a period of time and ζ is Coefficient of attenuation. A linear curve fitting could be used for acceleration of spectral intensity (ASI). As the ASI improved, the damage index increased linearly (Fig. 13). In this case, by increasing the ASI, the damage indices of higher structures were not greater necessarily.

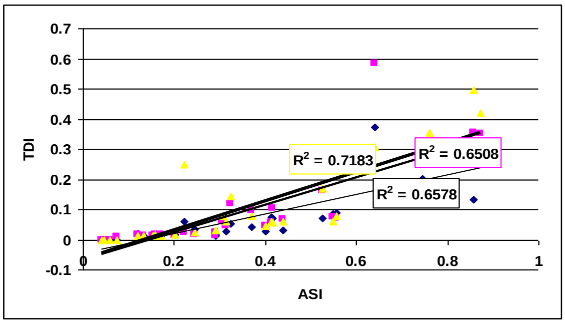

Fig. 13 Total Charts for damage index in ASI

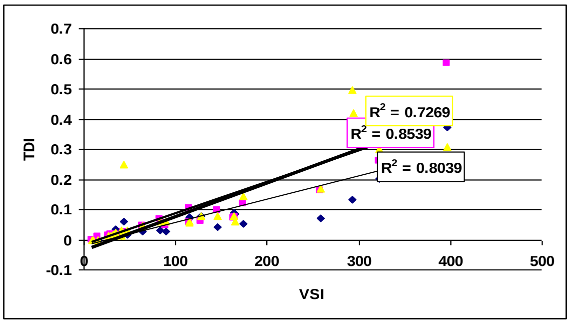

Fig. 14 Total Charts for damage index in VSI

$$ASI = \int_{0.1}^{0.5} S_a(\xi = 0.05, T)dT \qquad (11)$$

Velocity of Spectral intensity (VSI)

The calculation of the velocity of spectral intensity is shown in Eq.12. S_v is spectral acceleration; dT is a period of time and ζ is a coefficient of attenuation. A linear equation was sufficient for velocity spectral intensity. Fig. 13 shows when spectral velocity increased, the damage index increased linearly. This parameter was not sensitive to the height of the structures too.

$$VSI = \int_{0.1}^{2.5} S_v(\xi = 0.05, T)dT \qquad (12)$$

Sustained maximum acceleration (SMA)

In this case, sustained maximum acceleration was investigated (Steven L. Kramer 1996). None of the linear and nonlinear curve fittings were appropriate for correlating the damage index and maximum acceleration. In other words, according to Fig. 23, no specific relation could be found between damage index and maximum acceleration rate, especially in the longitudinal wave mode. In the case of transverse waves, the situation was slightly better, and the damage index increased with increasing maximum acceleration. In regard to the very low correlation coefficients, no specific effect could be found for the soil type too (Fig. 15).

Sustained maximum velocity (SMV)

According to Fig. 16, a linear equation was found for relating sustained maximum velocity (Steven L. Kramer 1996) and damage index. It is clear that the correlation

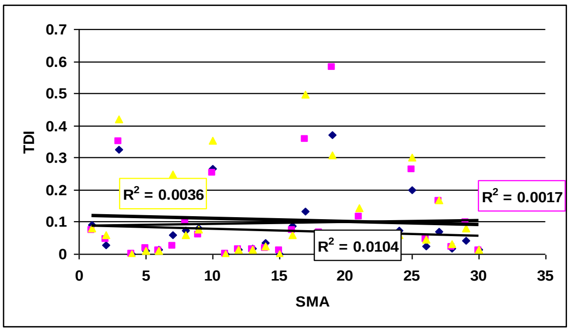

Fig. 15 Total Charts for damage index in SMA

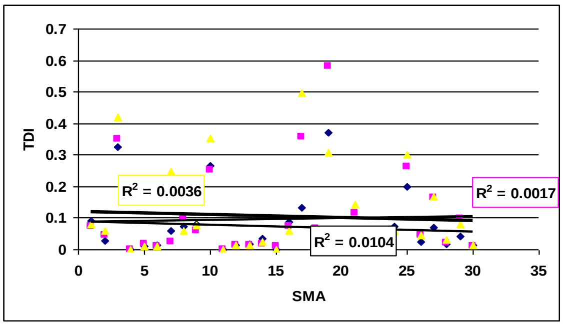

Fig. 16 Total Charts for damage index in SMV

coefficients are not acceptable. Nonlinear curve fitting could not improve the situation either. As the maximum speed increased, the damage index increased slightly. With increasing maximum velocity, the amount of damage in the taller structures was more than the shorter ones (Fig. 16).

Effective design acceleration (EDA)

Linear curve fitting was sufficient in effective design acceleration (Steven L. Kramer 1996) case. By changing the fitness curves to nonlinear ones, no better results were achieved. By increasing the effective design acceleration, the damage index increased linearly. By increasing the effective design acceleration, the amount of damage in the taller structures became more than the shorter ones (Fig. 17).

6.1.3 Correlation coefficients of earthquake parameters with damage index

The fitted curves in the previous section are used in this part, and the correlation coefficients are compared in Tables 12 and 13.

Most of the earthquake parameters had a linear relationship with damage index. In this case, peak ground acceleration and V_{max}/A_{max} had a second-degree relationship with this index. Therefore, these parameters were more important because, with a small change, damage changed more than the others.

Based on the analysis of results, peak ground velocity, characteristic intensity, Erias intensity, cumulative absolute velocity and velocity spectrum intensity had very good correlations with the damage index of the structures. To quantify the damages to the structures by the Park-Ang method, earthquake parameters that had very good correlations with damage index could minimize the time of

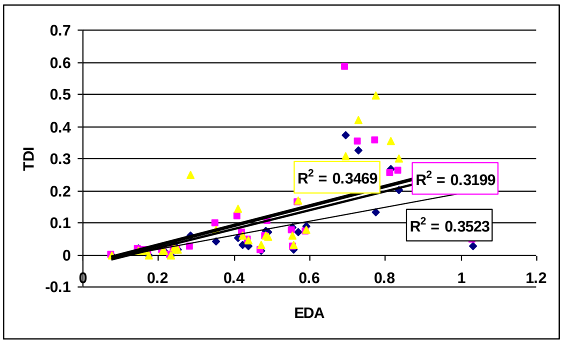

Fig. 17 Total Charts for damage index in EDA

Table 3 Correlation coefficient of earthquake parameters for building frames with different stories

Earthquake parameter	3-story frame	5-story frame	7-story frame
PGA	0.84	0.83	0.82
PGV	0.89	0.89	0.88
PGD	0.79	0.82	0.93
V_{max}/A_{max}	0.70	0.75	0.74
A_{rms}	0.37	0.28	0.32
V_{rms}	0.71	0.72	0.69
D_{rms}	0.09	.0.10	0.18
I_{Erias}	0.92	0.88	0.88
I_c	0.87	0.85	0.90
SED	0.73	0.79	0.69
CAV	0.82	0.82	0.91
ASI	0.81	0.81	0.85
VSI	0.89	0.93	0.85
SMA	0.59	0.57	0.59

the analysis of the structures (Tables 3 and 4).

The root mean square of displacement and effective design acceleration parameters had inappropriate correlations with Park-Ang damage index. Therefore, the parameters in the given order had better desirability for earthquake expressions.

According to the results of the study, another method was used. The purpose of the new method was to use a technique that increased the accuracy of the Park-Ang damage index as well as the speed of obtaining it. In the next section, the main earthquake waves were simulated with the particle swarm optimization (PSO) method to their equivalent sinusoidal waves.

6.2.1 Equivalent acceleration earthquakes with sinusoidal waves

In general, performing historical time analyzes requires, in the first place, basic accelerations by identifying the various parameters associated with strong ground motions. Therefore, the use of basic accelerations in such analyzes is difficult and time-consuming. Because all the parameters related to the acceleration of earthquakes may not always be readily available, researchers approached to the production of artificial accelerations to carry out time history analyses.

Table 4 Measurement of Correlation of Earthquake Parameters

Earthquake parameter	Measurement status	Total Correlation Coefficient (%)
PGA	Appropriate	86
PGV	Very appropriate	90
PGD	Appropriate	86
V_{max}/A_{max}	Appropriate	76
A_{rms}	Average	62
V_{rms}	Average	71
D_{rms}	Inappropriate	33
I_{Erias}	Very appropriate	91
I_c	Very appropriate	91
SED	Average	73
CAV	appropriate	89
SMA	Appropriate	85
SMV	Very appropriate	91

The method used in this research was to generate synthetic map accelerations using PSO algorithm; consequently, the acceleration of various earthquakes could be estimated with using simple sinusoidal functions. For this purpose, employing the PSO algorithm, the input data of the algorithm were 25 population, 3 times, the permissible error of $(0.001)^2$, the coefficients of personal and collective learning of 1.4192, and the coefficient of inertia of 0.7298. The accelerations of the various Iranian earthquakes described in the previous sections were replaced by a simple sinusoidal wave with the equation of $x= A\sin(\omega t)$. This waveform is the simplest produced synthetic acceleration that can be used as the initial input for dynamic time history analyses. Accordingly, in the present study, it is suggested that instead of using accelerated mapping with high dependent parameters for dynamic analysis, equivalent sinusoidal waves can be used that are dependent on only two variables of A and ω. In fact, only by precise determination of these two parameters, one can find logical answers to the analysis of the damages of reinforced concrete structures.

For this purpose, the effective parameters in the production of sinusoidal wave equivalent to A and ω were considered as optimization variables. In the next step, using the trial and error method, the best range was determined for these two variables, and it was determined that the ranges obtained were largely in line with the range of the amplitude and frequency of the main earthquake. In other words, it can be said that by applying the above method and determining the range of amplitude and frequency variations between zero and dominant frequencies of the earthquake, sinusoidal waves could be found to the acceleration of the initial earthquakes.

In the Table 5, the acceleration time for each earthquake and the time steps used in the analysis are presented to estimate the equivalent sinusoidal waves. In addition, in this table, the amplitude and frequency range of each earthquake is presented for the acceleration of the longitudinal and transverse waves of each earthquake.

6.2.2 Optimization steps by PSO

In general, accelerations are complex graphs that represent the values in a period of time. Such complex forms cannot be simplified without neglecting some of their basic characteristics. All parameters, which are related to the acceleration of an earthquake, may not always be available easily. In this study, it is tried to provide a sinusoidal wave equivalent to the acceleration. Obviously, the equivalent sinusoidal waves and accelerations cannot be compared to each other directly, and it is necessary to do so after the initial simplifications. For this purpose, the parameters must be used, which are appropriate representatives for measuring the equivalent sinusoidal waves and accelerating the initial earthquakes. In this regard, a tool represents the effects of earthquakes on structures, such as the amount of damages of them, is very convenient for studying the behavior of structures.

In this study, the damage index method is used to compare the feasibility of equivalent synthetic wave productions that can have the same basic earthquake characteristics. In other words, the damage index produced by the presented accelerations was used for RC structures. The damage index actually represents the behavior of structures under earthquakes within the high performance ranges and expresses the damages of structures by possible earthquakes. Therefore, this parameter can be a suitable tool for a comprehensive comparison of structural behavior in the two different situations. In fact, the damage indices produced by earthquakes and the generated sinusoidal waves are compared in this research.

In this research, at first the magnitude of the earthquake damage indices were calculated; afterwards, different sinusoidal waves were generated produced the equivalent damage indices. In fact, by finding the best values for sinusoidal variables, which were A and ω, this algorithm worked. In other words, by performing dynamic analysis, the equivalent damage indices of all sinusoidal waves were determined and compared with the magnitude of the damage indices obtained from the main earthquake. Meanwhile, the difference between the damage index of the major earthquake and the damage index due to the sinusoidal waves were determined and considered as cost in the optimization algorithm. This trend should be continued to reach the optimal response, and thus the variable values, which were found for the equivalent sinusoidal waves, were considered as the best parameters of the sinusoidal waves representing the main earthquakes.

6.2.3 Equivalent results of accelerated earthquakes with sinusoidal waves

Table 5 is to show the sinusoidal functions equivalent to the longitudinal and transverse waves of the various earthquakes presented earlier. First, the three, five, and seven story structures were modeled in IDARC software. Then, they were subjected to the longitudinal and transverse earthquake waves in both soil types 1 and 2. Actually, dynamic time history analyses were completed, and the damage index resulting from each earthquake was obtained. As shown in Tables 6 to 11, each of these accelerations was replaced with an equivalent sinusoidal wave. It should be

Table 5 Amplitude and frequency range of longitudinal and transverse waves of selected earthquakes accelerations

Earthquake		Frequency range(Hrz)	Amplitude range (mm)	Time step (s)	Duration(s)
Tabas	Longitudinal	0-1.5138	0-0.213	0.005	19
	Transverse	0-4.1922	0.-0.28	0.005	19
Aab bar	Longitudinal	0-6.3	0-0.249	0.005	30
	Transverse	0-6.18	0-0.287	0.005	30
Vandik	Longitudinal	0-4.3	0-0.312	0.005	32.5
	Transverse	0-4.105	0-0.262	0.005	32.5
Naghan	Longitudinal	0-3.175	0-0/213	0.005	32.5
	Transverse	0-4.19922	0-0/484	0.005	32.5
Avaj	Longitudinal	0-10.95	0-0.327	0.005	32.5
	Transverse	0-10.084	0-0.394	0.005	32.5
Chalan cholan	Longitudinal	0-2.923	0-0.431	0.005	32.5
	Transverse	0-2.31934	0-0.357	0.005	32.5

Table 6 Equivalent damage caused by sinusoidal wave equivalent to Tabas earthquake acceleration

ω		A		Equivalent damage		Damage		Levels
Transvers	Longitudinal	Transvers	longitudinal	Transvers	Longitudinal	Transvers	longitudinal	
4.2805	3.2817	0.08242	0.070346	0.015	0.013	0.015	0.011	3
1.0176	0.83559	0.11538	0.13356	0.014	0.014	0.015	0.016	5
0.53017	0.10056	0.12424	0.17517	0.015	0.014	0.015	0.012	7

Table 7 Equivalent damage caused by sinusoidal wave equivalent to Aab bar earthquake acceleration

ω		A		Equivalent damage		Damage		Levels
Transvers	Longitudinal	transvers	Longitudinal	Transvers	longitudinal	Transvers	longitudinal	
7.23	5.114	0.03898	0.58451	0.016	0.015	0.017	0.013	3
3.1218	3.1218	0.10845	0.10845	0.013	0.017	0.014	0.011	5
0.4618	1.9819	0.10918	0.13495	0.012	0.011	0.015	0.011	7

noted that PSO optimization algorithm was used to simulate accelerations in the form of a sinusoidal wave, and the parameters of amplitude *A* and frequency ω were obtained. Subsequent frames were studied again with using the sinusoidal wave under nonlinear dynamic analysis, and the equivalent damage indices were determined. Each of the shapes had two parts of A and B, respectively, which were the longitudinal and transverse acceleration components of the various earthquakes. The damage index values resulting from the longitudinal and transverse components of the earthquakes and the equivalent damage indices of the sinusoidal waves can be seen here too.

Based on the results, in all earthquakes, the estimated damage indices according to the equivalent sinusoidal waves showed a fairly good agreement with the ones caused by the real longitudinal and transverse components of the earthquakes in both soil types 1 and 2. The results of the diagrams show that the compliance rate between the damage indices caused by the acceleration of the main earthquakes and sinusoidal waves was about 95%. The effects of soil type were not considerable in the results of this research. It means, the matching rates in the responses of time history analyses were very high based on the magnitude of the earthquake accelerations and the equivalent sinusoidal waves in both soil types. Also, in both soils, as the number of stories increased, the amplitude of the waves increased and the frequency of them decreased.

At a constant time interval, the interaction of amplitude and frequency of earthquake waves and sinusoidal waves were studied too. The results showed these two parameters had inverse relationships. In fact, in a fixed algorithm, with increasing the number of floors, the equivalent sinusoidal amplitude increased and the frequency decreased. It is worth noting that by using the sinusoidal wave equivalent to the accelerations of the original earthquakes, the time consuming of the nonlinear dynamical analysis was reduced by almost half in all circumstances.

6.2.4 Matching the sinusoidal functions to the other RC frames

In this section, in order to determine the equivalent sinusoidal waves, the first-order equation for sinusoidal wave coefficients (range of amplitude A and frequency ω) were obtained using curve fitting method. Each of these linear equations for amplitude and frequency in each earthquake was determined with the number of frame stories (x). Because the correlation coefficients (R^2) of all the graphs were more than 0.8, the results of curve fittings

Table 8 Equivalent damage caused by sinusoidal wave equivalent to Vandik earthquake acceleration

ω		A		Equivalent damage		Damage		Levels
Transvers	Longitudinal	transvers	Longitudinal	Transvers	longitudinal	Transvers	longitudinal	
3.01	3.765	0.13948	0.10209	0.043	0.022	0.047	0.021	3
0.82847	1.9819	0.13952	0.13495	0.016	0.027	0.017	0.027	5
0.31231	0.73094	0.15431	0.17701	0.02	0.05	0.024	0.04	7

Table 9 Equivalent damage caused by sinusoidal wave equivalent to Naghan earthquake acceleration

ω		A		Equivalent damage		Damage		Levels
Transvers	Longitudinal	transvers	Longitudinal	Transvers	Longitudinal	Transvers	Longitudinal	
2.6628	4.059	0.12482	0.092532	0.021	0.021	0.019	0.019	3
1.6	2.8	0.13785	0.15515	0.016	0.016	0.016	0.016	5
0.90114	0.16581	0.13942	0.21184	0.015	0.017	0.016	0.016	7

Table 10 Equivalent damage caused by sinusoidal wave equivalent to Avaj earthquake acceleration

ω		A		Equivalent damage		Damage		Levels
Transvers	Longitudinal	transvers	longitudinal	transvers	longitudinal	Transvers	Longitudinal	
1.2685	1.4189	0.18277	0.18855	0.023	0.037	0.026	0.031	3
0.42882	0.52776	0.18423	0.19676	0.048	0.069	0.044	0.067	5
0.37325	0.45057	0.19913	0.2	0.049	0.060	0.046	0.059	7

Table 11 Equivalent damage caused by sinusoidal wave equivalent to Chalan cholan earthquake acceleration

ω		A		Equivalent damage		Damage		Levels
transvers	longitudinal	transvers	longitudinal	transvers	longitudinal	Transvers	longitudinal	
1.58	2.8905	0.16746	0.18321	0.044	0.050	0.043	0.054	3
0.62905	0.6	0.24852	0.19635	0.069	0.14	0.068	0.113	5
0.1089	0.59	0.2626	0.21	0.08	0.144	0.08	0.144	7

were acceptable. Therefore, for simplicity in calculations, these functions were used to estimate the amplitude and frequency values of the sinusoidal functions. The purpose of this work was to estimate the amplitude and frequency, and consequently the sinusoidal waves equivalent to the various earthquakes in four and six story frames.

After determining the sinusoidal waves equivalent to various earthquakes, the damage indices caused by the earthquakes in four and six floor buildings were determined using IDARC software. The selected time steps were 0.005 second, and the maximum total time of analysis was 32.5 seconds. It is worth reminding that instead of using the accelerations of the main earthquakes for time history analyses, the equivalent sinusoidal waves were used. To validate the results of equivalent damage indices caused by sinusoidal waves in four- and six-story frames, the damageindices of these frames were determined according to the real longitudinal and transverse components of the earthquakes too. The results of this part are presented in Tables 12 and 13. By comparing the damage indices achieved in these two methods, it can be seen that the results were approximately the same. It means, the method presented in this study the ability to estimate the damage index of middle height RC frames properly.

In general, using sinusoidal waves to determine the damage indices of structures was better than earthquake parameters. Also the time of analysis with the sinusoidal waves was about 65% of the time with the earthquake parameters.

7. Conclusions

The summery of the results gained in this research are:

- Most of the earthquake parameters had linear relationships with damage indices. In this case, peak ground acceleration and V_{max}/A_{max} had a quadratic relationship with them. Therefore, these parameters were the most important ones in this case, and with a small change in them, the damage indices altered considerably compared to the others.
- Peak ground velocity, characteristic intensity, Erias intensity, cumulative absolute velocity and velocity spectrum intensity had very good correlations, which were about 90 percent, with the damage indices of the structures. To quantify the damages of the structures using the Park-Ang method, earthquake parameters that had very good correlations with damage indices could minimize the time of the analysis of the structures.
- The root mean square of displacement and effective design acceleration parameters had inappropriate correlations with Park-Ang damage indices.
- In time history analysis, the differences among the damage indices due to the acceleration of major

Table 12 The values of the sinusoidal coefficients equivalent to the longitudinal and transverse components of the earthquakes.

Accelerated station	Longitudinal	Transvers
Hashtpar	A= 0.0298x+0.004	A= 0.0037x+0.1158
	ω= -0.9933x+7.2081	ω= -0.4404x+3.9234
Firooz abad	A= 0.0262x-0.0047	A= 0.0105x+0.0551
	ω= -0.7953x+5.3824	ω= -0.9376x+6.6307
Zaraat	A= 0.087x+0.0444	A= 0.0037x+0.1259
	ω= -0.5841x+4.8475	ω= -0.6744x+4.7557
Avaj	A=0.0029x+0.1808	A= 0.0041x+0.1683
	ω= -0.2421x+2.0095	ω= -0.2238x+1.8093
Koshak	A= 0.0191x+0.005	A= 0.0175x+0.005
	ω= -0.783x+7.321	ω= -1.6921x+12.065
Chalan cholan	A= 0.0067x+0.163	A= 0.0238x+0.1073
	ω= -0.5751x+4.2385	ω= -0.3678x+2.6115

Table 13 The values of amplitude and frequency correlation coefficients of sinusoidal waveform equivalent to longitudinal and transverse acceleration

Accelerated station	Longitudinal		Transvers	
	A	ω	A	ω
Hashtpar	0.992	0.9601	0.8296	0.986
Firoozabad	0.986	0.912	0.9003	0.845
Zaraat	0.995	0.9983	0.752	0.8873
Avaj	0.9414	0.8094	0.8164	0.7964
Koshak	0.9695	0.9759	0.7578	0.985
Chalan cholan	0.9999	0.7533	0.8582	0.9722

earthquakes and equivalent sinusoidal waves were up to 5 percent. Therefore, the equivalent sinusoidal waves can be used instead of the main accelerations in the calculation of damage indices.

- The soil type did not have considerable effects on the sinusoidal waveguide algorithm. In fact, without regarding the type of soil, the damage indices of structures could be obtained with using PSO-equivalent sinusoidal waves.
- Using sinusoidal waves was more user friendly than earthquake parameters to determine the damage indices of the structures. Also, the time of analysis with the sinusoidal waves was about 65% of the one with earthquake parameters

References

Alvanitopoulos P.F., Andreadis I. and Elenas A. (2010) “Interdependence between damage indices and ground motion parameters based on Hilbert–Huang transform”, *Measure. Sci. Technol.*, **21**(2), 025101-025115. https://doi.org/10.1088/0957-0233/21/2/025101.

Artar M. (2016), “Optimum design of steel space frames under earthquake effect using harmony search” *Struct. Eng. Mech.*, **58**(3), 597-612. https://doi.org/10.12989/sem.2016.58.3.597.

Banon H., Veneziano D. (1982), “Seismic safety of reinforced concrete members and structures”, *Earthq. Eng. Struct. Dynam.*, **10**(2), 179-193. https://doi.org/10.1002/eqe.4290100202.

Bas S. and Kalkan I. (2016), “The effects of vertical earthquake motion on a R/C structure”, *Struct. Eng. Mech.*, **59**(4), 719-737. https://doi.org/10.12989/sem.2016.59.4.719.

Basack S. and Nimbalkar S. (2017), “Free strain analysis of the performance of vertical DRAINs for soft soil improvement”, *Geomech. Eng.*, **13**(6), 963-975. https://doi.org/10.12989/gae.2017.13.6.963.

BHRC (2017), Building and Housing Research Center, Ministry of Roads and City Planning, Tehran, Iran. www.bhrc.ac.ir

Cabanas L., Bonito B. and Herraiz M. (1997), “An Approach for theMeasurement of the Potential Structural Damage of Earthquake Ground Motions”, *Earthq. Eng. Struct. Dynam.*, 26(1), 79-92. https://doi.org/10.1002/(SICI)1096-9845(199701)26:1%3C79::AID-EQE624%3E3.0.CO;2-Y.

Cantagallo, C., Camata, G. and Spacone, E. (2019) “A Probability-based Approach for the Definition of the Expected Seismic Damage Evaluated with Non-linear Time-History Analyses”, *J. Earthq. Eng.*. **23**(2), 261-283. https://doi.org/10.1080/13632469.2017.1323043.

Cantagallo,C., Camata, G. and Spacone, E. (2019) “A probability-based approach for the definition of the expected seismic damage evaluated with non-linear time-history analyses”, *J. Earthq. Eng.*, **23**(2), 261-283. https://doi.org/10.1080/13632469.2017.1323043.

Cao V. and Raonagh H. (2014), “Correlation between seismic parameters of far-fault motions and damage indices of low-rise reinforced concrete frames”, *Soil Dynam. Earthq. Eng.*, **66**, 102-112. https://doi.org/10.1016/j.soildyn.2014.06.020.

Chatterjee S., Sarkar S., Hore S., Dey N., Ashour A. and Balas V. (2016), “Particle swarm optimization trained neural network for structure failure prediction of multistoried RC buildings", *Neural Comput. Appl.,* **28**(8), 2005–2016. https://doi.org/10.1007/s00521-016-2190-2.

Chen j., Shu W. and Huang H. (2017), "Rate-dependent progressive collapse resistance of beam-to-column connections with different seismic details", *J. Perform. Construct. Facilities*, **31**(2). https://doi.org/10.1061/(ASCE)CF.1943-5509.0000922.

Chen Z. and Yu L. (2017), "A novel pso-based algorithm for structural damage detection using Bayesian multi-sample objective function", *Struct. Eng. Mech.*, **63**(6), 825-835. https://doi.org/10.12989/sem.2017.63.6.825.

Chen Z., Shi C., Li T. and Yuan Y. (2012), "Damage characteristic and influence factors of mountain tunnels under strong Earthquakes", *Natural Hazards,* **61**(2), 387-401. https://doi.org/10.1007/s11069-011-9924-3.

Chen, Z. and Yu, L. (2017), "A novel PSO-based algorithm for structural damage detection using Bayesian multi-sample objective function", *Struct. Eng. Mech.*, **63** (6), 825-835. https://doi.org/10.12989/sem.2017.63.6.825.

Colombo A. and Negro P. (2005), "A damage index of generalized applicability", *Eng. Struct.*, **27**(8), 1164-1174. https://doi.org/10.1016/j.engstruct.2005.02.014.

Elenas A. (1997), "Interdependency between seismic acceleration Parameters and the behaviour of structures", *Soil Dynam. Earthq. Eng.*, **16**(5), 317–322. https://doi.org/10.1016/S0267-7261(97)00005-5.

Elenas A. (2000), "Correlation between seismic acceleration parameters and overall structural damage indices of buildings", *Soil Dynam. Earthq. Eng.,* **20**(1), 93-100. https://doi.org/10.1016/S0267-7261(00)00041-5.

Elenas A. and Liolios A. (1995), "Earthquake induced nonlinear behavior of reinforced concrete frame structures in relation with characteristic acceleration parameters", *Proceedings of the 5th International Conference on Seismic Zonation*, Nice, October.

Elenas A. and Meskouris K. (2001), "Correlation study between seismic acceleration parameters and damage indices of structures", *Eng. Struct.,* **23**(6), 698–704. https://doi.org/10.1016/S0141-0296(00)00074-2.

Elenas A., Liolios A. and Vasiliadis L. (1995), "Earthquake Induced nonlinear behavior of structures in relation with characteristic acceleration parameters", *Proceedings of the 10th European conference on earthquake engineering*, Vienna, August.

Erdem H. (2010), "Prediction of moment capacity of reinforced concrete slabs in fire using artificial neural networks", *Adv. Eng. Software*, **41**(2), 270–276. https://doi.org/10.1016/j.advengsoft.2009.07.006.

Federal Emergency Management Agency (2000), Prestandard and commentary for the seismic rehabilitation of buildings: FEMA-356, Washington (DC), USA.

Habibi, A., Izadpanah, M. (2017), "Improving the linear flexibility distribution model to simultaneously account for gravity and lateral loads", *Comput. Concrete*, **20** (1), 11-22. https://doi.org/10.12989/cac.2017.20.1.011.

Habibi, A.., Izadpanah, M. (2012), "New method for the design of reinforced concrete moment resisting frames with damage control", *Scientia Iranica*, **19**(2), 234-241. https://doi.org/10.1016/j.scient.2012.02.007.

Habibi, A.Jami,E. (2017), "Correlation between ground motion parameters and target displacement of steel structures", *J. Civil Eng.*, 15, 163-174. https://doi.org/10.1007/s40999-016-0084-4.

Habibi, A.R., Izadpanah, M., Yazdani, A. (2013), "Inelastic damage analysis of RCMRFs using pushover method", *Iran. J. Sci. Technol.*, 37(C2), 345-352.

Habibi,A. and Asadi, K. (2017), "Development of drift-based damage index for reinforced concrete moment resisting frames with setback", *J. Civil Eng.*, 37(2),345-352. https://doi.org/10.1007/s40999-016-0085-3.

Hajela P. and Berke L. (1991), "Neurobiological computational models in structural analysis and design", *Comput. Struct.*, **41**(4), 657–667. https://doi.org/10.1016/0045-7949(91)90178-O.

Housner G. W. and Jennings P. C. (1964), "Generation of artificial earthquakes", *J. Eng. Mech. Division*, **90**(1), 113-152.

Izadpanah, M., Habibi, A. (2018), "New spread plasticity model for reinforced concrete structural elements accounting for both gravity and lateral load effects", *J Struct. Eng. ASCE*, **144**(5): 04018028. https://doi.org/10.1061/(ASCE)ST.1943-541X.0002016.

Izadpanaha M. and Habibi A. (2015), "Evaluating the spread plasticity model of IDARC for inelastic analysis of reinforced concrete frames", *Struct. Eng. Mech.*, 56(2), 169-188. https://doi.org/10.12989/sem.2015.56.2.169.

Jakubek M. (2017), "Neural network prediction of load capacity for eccentrically loaded reinforced concrete columns", *Computer Assisted Methods Eng. Sci.*, **19**(4), 339–349. https://cames.ippt.pan.pl/index.php/cames/article/view/84.

Kappos A. J. (1997), "Seismic damage indices for RC buildings: evaluation of concepts and procedures", *Struct. Eng. Mater.*, **1**(1), 78-87. https://doi.org/10.1002/pse.2260010113.

Karamloo, M., Mazloom, M. and Payganeh, G. (2017) "Effect of size on nominal strength of self-compacting lightweight concrete and self-compacting normal weight concrete: A stress-based approach", *Mater. Today Communications*, **13**, 36-45. https://doi.org/10.1016/j.mtcomm.2017.08.002.

Kennedy J. and Eberhart R. (1995), "Particle Swarm Optimization," *Proceeding of the IEEE International Conference on Neural Networks*, Perth, November.

Kim H. and Chung C. (2016), "Integrated system for site-specific earthquake hazard assessment with geotechnical spatial grid information based on GIS", *Natural Hazards*, **82**(2), 981-1007. https://doi.org/10.1007/s11069-016-2230-3.

Lagaros N. D., Papadrakakis M. (2012), "Neural network based prediction schemes of the non-linear seismic response of 3D buildings", *Adv. Eng. Software*, **44**(1), 92–115. https://doi.org/10.1016/j.advengsoft.2011.05.033.

Massumi A. and Gholami F (2016), "The influence of seismic intensity parameters on structural damage of RC buildings using principal components analysis", *Appl. Math. Model.*, **40**(3), 2161-2176. https://doi.org/10.1016/j.apm.2015.09.043.

Mazloom, M. and Mahboubi, F. (2017), "Evaluating the settlement of lightweight coarse aggregate in self-compacting lightweight concrete", *Comput. Concrete,* **19**(2), 203-210. https://doi.org/10.12989/cac.2017.19.2.203.

Mazloom, M. and Ranjbar, A. (2010), "Relation between the workability and strength of self-compacting concrete", *35th Conference on Our World in concrete & Structures*, Singapore, August.

Mazloom, M., Saffari, A. and Mehrvand, M. (2015) "Compressive, shear and torsional strength of beams made of self-compacting concrete", *Comput. Concrete,* **15**(6), 935-950. https://doi.org/10.12989/cac.2015.15.6.935.

Mirzai, N., Zahrai, M. and Bozorgi, F. (2017), "Proposing optimum parameters of TMDs using GSA and PSO algorithms for drift reduction and uniformity", *Struct. Eng. Mech.*, **63**(2), 147-160. https://doi.org/10.12989/sem.2017.63.2.147.

Mohebi, B., Chegini, A. and Miri. A. (2019), "A new damage index for steel MRFs based on incremental dynamic analysis", *J. Construct. Steel Res.*, **156**, 137-154. https://doi.org/10.1016/j.jcsr.2019.02.005.

Ozmen H. B. and Inel M. (2016), "Damage potential of earthquake records for RC building stock", *Earthq. Struct.*, **10**(6), 1315-1330. http://dx.doi.org/10.12989/eas.2016.10.6.1315.

Park Y. J. and Ang A. H. S. (1985), "Mecha nistic Seismic Damage Model for Reinforced Concrete", *J. Struct. Eng. ASCE*, 111(4), 722-739. https://doi.org/10.1061/(ASCE)0733-9445(1985)111:4(722).

Park Y. J., Ang A. H. S. and En Y. W. W. (1988), "Seismic damage analysis of reinforced concrete buildings", *Proceedings of 9th world Conference on Earthquake Engineering,* Tokyo-Kyoto ,August.

Plevris V. and Papadrakakis M. (2011), "A hybrid particle swarm-gradient algorithm for global structural optimization", *Computer-Aided Civil Infrastruct. Eng.*, **26**(1), 48–68. https://doi.org/10.1111/j.1467-8667.2010.00664.x.

Rahman M. S., Chang S. and Kim D. (2017), "Multiple wall dampers for multi-mode vibration control of building structures under earthquake excitation", *Struct. Eng. Mech.*, **63**(4), 537-549. https://doi.org/10.12989/sem.2017.63.4.537.

Roudak M., and Karamloo, M. (2019), "Establishment of non-negative constraint method as a robust and efficient first-order reliability method", *Appl. Math. Model.*, **68**, 281-305. https://doi.org/10.1016/j.apm.2018.11.021.

Roudak, M., Shayanfar, M. and Karamloo, M. (2018), "Improvement in first-order reliability method using an adaptive chaos control factor", *Structures*, **16**, 150-156. https://doi.org/10.1016/j.istruc.2018.09.010.

Roudak, M., Shayanfar, M., Barkhordari, M. and Karamloo, M. (2017), "A robust approximation method for nonlinear cases of structural reliability analysis", *J. Mech. Sci.*, **133**, 11-20. https://doi.org/10.1016/j.ijmecsci.2017.08.038.

Roudak, M., Shayanfar, M., Barkhordari, M. and Karamloo, M. (2017), "A new three-phase algorithm for computation of reliability index and its application in structural mechanics", *Mech. Res. Communications*, **85**, 53-60. https://doi.org/10.1016/j.mechrescom.2017.08.008.

Shayanfar, M., Barkhordari, M. and Roudak, M. (2018), "A new effective approach for computation of reliability index in nonlinear problems of reliability analysis", *Communications in Nonlinear Sci. Numeric. Simulation,* **60**, 184-202. https://doi.org/10.1016/j.cnsns.2018.01.016.

Standard No. 2800-05 (2015), Iranian Code of Practice for seismic Resistant Design of Buildings, Building and Housing Research Center, Tehran, Iran.

Steven L. Kramer (1996), *Geotechnical Earthquake Engineering*, Prentice-Hall International Series in Civil Engineering and Engineering Mechanics, Upper Saddle River, New Jersey, USA.

Valles R. E., Reinhorn A. M., Kunnath S. K., Li C. and Madan A. (1996), *IDARC2D, Version 4.0: A Computer Program for the Inelastic Damage Analysis of Buildings*, National Center for Earthquake Engineering Research, New York, NY, USA.

Vui V. C., Raonagh H. R. (2014), "Correlation between seismic parameters of far-fault motions and damage indices of low-rise reinforced concrete frames", *Soil Dynam. Earthq. Eng.,* **66**, 102-111. https://doi.org/10.1016/j.soildyn.2014.06.020.

Zarghami, E., Azemati, H., Fatourehchi, D. and Karamloo, M. (2018), "Customizing well-known sustainability assessment tools for Iranian residential buildings using Fuzzy Analytic Hierarchy Process", *Building and Environment,* **128**, 107-128. https://doi.org/10.1016/j.buildenv.2017.11.032.

Zarghami, E., Fatourehchi, D. and Karamloo, M. (2017), "Impact of daylighting design strategies on social sustainability through the built environment", *Sustainable Development*, **25**(6), 504–527. https://doi.org/10.1002/sd.1675.

CC